

A Non-Self-Adjoint Finite Difference Model of Electron Diffusion Parallel to Electric Fields

C. A. HALL* AND J. J. LOWKE

Westinghouse Research Laboratories, Pittsburgh, Pennsylvania 15235

Received January 31, 1975; revised May 22, 1975

The electron distribution function plays a key role in the quantitative study of various properties of electrons moving through a gas and is characterized as a solution of the Boltzmann transport equation. Simplification of this model results in a non-self-adjoint second-order elliptic partial differential equation with variable coefficients. The complexity of the coefficients precludes the use of a coordinate transformation to remove second-order cross-derivative terms, and the nonmodelness of the boundary value problem necessitates rather novel applications of various tools of numerical analysis for successful solution. Due to the non-self-adjointness, any consistent finite difference model is bound to be nonsymmetric; however, a finite difference scheme is devised which is "almost symmetric." Iterative solution of the resulting difference equations is analyzed and an acceleration strategy for convergence is devised. Numerical results are included for a typical problem involving in excess of 5000 Mesh points. This problem was solved on the UNIVAC 1106 in less than 6 min of CPU time.

1. INTRODUCTION

Electron drift and diffusion in a gas under the influence of an electric field are conventionally described [1, 2] in terms of the distribution function $f^0(\mathbf{r}, \epsilon)$ where $f^0(\mathbf{r}, \epsilon) \epsilon^{1/2} d\epsilon d\mathbf{r}$ is proportional to the number of electrons at \mathbf{r} in $d\mathbf{r}$ having electron energy between ϵ and $\epsilon + d\epsilon$. The function f^0 is the first term of a two-term spherical harmonics expansion in velocity space of the distribution function $f(\mathbf{r}, \mathbf{v})$, where $f(\mathbf{r}, \mathbf{v}) d\mathbf{r} d\mathbf{v}$ denotes the number of electrons at position \mathbf{r} in volume $d\mathbf{r}$ and with velocity \mathbf{v} in the range $d\mathbf{v}$. These functions are discussed more fully in Section 2 and are defined by the Boltzmann transport equation.

It has been usual to obtain numerical or analytic solutions of f^0 as a function of energy by ignoring all terms involving derivatives in the Boltzmann equation with respect to r , i.e., solutions are obtained for a spatially uniform distribution of electrons [3]. The derived function f^0 is then usually used to derive diffusion coefficients and drift velocities which are applied to physical situations where the

* Mathematics Department, University of Pittsburgh, Pittsburgh, Pa. 15260.

electron distribution is not spatially uniform [4]. Such analyses of experimental observations in uniform electric fields of diffusion coefficients and drift velocities have led to the successful derivation of electron collision cross sections, as a function of energy, for most common gases [2, 3].

However, as diffusion coefficients are a function of f^0 , they are also strictly a function of \mathbf{r} , even in a uniform electric field. It has been shown previously that the spatial gradient terms in the Boltzmann equation lead to significant physical effects, for example, the width of a diffusing electron pulse can differ by more than a factor of 2 from that given by the conventional theory [5, 6].

In the present paper a numerical method is described to solve the Boltzmann equation in f^0 , where the gradient terms in r are retained. In the numerical example presented in Section 5 we consider the physical situation of a steady stream of electrons drifting under the influence of a uniform electric field and being absorbed by a metal boundary. The distance from the boundary over which the electron density and velocity distribution are perturbed is large compared with the mean free path of electrons between collisions with gas molecules, e.g., for the example discussed later in Fig. 3, the effect of the absorbing electrode extends 0.5 cm from the electrode whereas the mean free path is 0.008 cm. Thus we still assume the validity of the two-term spherical harmonics expansion. However, for the large-density gradients which occur near an absorbing boundary, this assumption may not be a valid approximation, in which case the problem would need to be further examined by, for example, Monte Carlo methods [7].

The present paper is concerned largely with the numerical methods used. The physical significance of the results that are obtained for various cross sections will be discussed in a later paper.

2. BOLTZMANN THEORY AND GOVERNING EQUATIONS

The general electron distribution function, $f(\mathbf{r}, \mathbf{v}, t)$, plays a key role in the quantitative study of electrons moving through a gas and is characterized as a solution of the Boltzmann transport equation [1, 2]. The quantity $f(\mathbf{r}, \mathbf{v}, t) d\mathbf{r} d\mathbf{v}$ denotes the number of electrons at position \mathbf{r} in volume $d\mathbf{r}$ and with velocity \mathbf{v} in the range $d\mathbf{v}$, both at time t . In order to simplify the Boltzmann equation it is usually assumed that the distribution function f is almost spherically symmetric in velocity space and hence it is adequately represented by the first two terms of an expansion in spherical harmonics, i.e.,

$$f(\mathbf{r}, \mathbf{v}, t) = f^0(\mathbf{r}, \epsilon, t) + f^1(\mathbf{r}, \epsilon, t) \cos \theta, \quad (1)$$

where ϵ is the electron energy and θ is the angle between \mathbf{v} and the direction of the

electric field. In the case of elastic collisions the fractional energy gain or loss by an electron upon colliding with a gas atom is small and this assumption (1) is very accurate [8].

By integrating the Boltzmann equation over (i) $d\theta$ and (ii) $\cos \theta d\theta$, two partial differential equations in f^0 and f^1 are obtained from which f^1 can be eliminated to obtain the equation

$$\begin{aligned} & \frac{4\pi}{m} \left(\frac{2\epsilon}{m}\right)^{1/2} \frac{\partial f^0}{\partial t} \\ &= \frac{16\pi}{mM} \frac{\partial}{\partial \epsilon} \left[N\epsilon^2 Q \left(f^0 + kT \frac{\partial f^0}{\partial \epsilon} \right) + \frac{MeE}{6mN} \frac{\epsilon}{Q} \left(eE \frac{\partial f^0}{\partial \epsilon} + \frac{\partial f^0}{\partial z} \right) \right] \\ &+ \frac{8\pi}{3m^2N} \frac{\epsilon}{Q} \left(eE \frac{\partial^2 f^0}{\partial \epsilon \partial z} + \frac{\partial^2 f^0}{\partial z^2} \right), \end{aligned} \tag{2}$$

which defines f^0 [5, Eq. (17)]. This equation can be rearranged to the form

$$\frac{4\pi}{m} \left(\frac{2\epsilon}{m}\right)^{1/2} \frac{\partial f^0}{\partial t} = \nabla \cdot (B \nabla f^0) + d_1 \frac{\partial f^0}{\partial \epsilon} + d_2 \frac{\partial f^0}{\partial z} + d_3 f^0, \tag{3}$$

where

- m is the electron mass,
- ϵ is the electron kinetic energy,
- ∇ is the gradient operator $[(\partial/\partial\epsilon)(\partial/\partial z)]^T$,
- B is a 2×2 matrix,

$$B = \frac{8\pi\epsilon}{3m^2NQ} \begin{bmatrix} e^2 E^2 + (6mN^2\epsilon QkT/M) & eE \\ eE & 1 \end{bmatrix} \tag{4}$$

- z is the distance along a given direction of propagation,
- $n(z)$ is the total number density $N\alpha P$ (293/T),
- P, T are the pressure and temperature of the gas,
- $Q(\epsilon)$ is the momentum transfer cross section,
- e is the electron charge, (5)
- $E(z)$ is the magnitude of the electric field $\mathbf{E} = Ek$, \mathbf{k} a unit vector along the z -axis,
- M is the atomic mass of the gas,
- k is the Boltzmann constant.

$$d_1 = \frac{16N\pi}{mM} \epsilon^2 Q - \frac{8\pi\epsilon}{3m^2Q} \frac{\partial E}{\partial z} \frac{1}{N}, \tag{6}$$

$$d_2 = -\frac{8\pi\epsilon}{3m^2Q} \frac{\partial}{\partial z} \frac{1}{N}, \quad d_3 = \frac{\partial d_1}{\partial \epsilon}. \tag{7}$$

It is of value to examine the relative magnitudes of the above quantities, i.e., $m \sim 10^{-27}$, $N \sim 10^{17}$, $M \sim 10^{-24}$, $e \sim 10^{-19}$, $P \sim 1$, $E \sim 1$, $Q \sim 10^{-15}$, and $k \sim 10^{-16}$. Hence the matrix of coefficients

$$B \sim \epsilon \begin{bmatrix} 10^{14} + 10^{37} \epsilon T & 10^{33} \\ 10^{33} & 10^{52} \end{bmatrix}, \quad (8)$$

$d_1 \sim 10^{54} \epsilon^2$, etc. We found it computationally convenient to scale the independent variable, energy, by

$$\epsilon = \epsilon / (10^7 e), \quad (9)$$

so that ϵ is now in electron volts, and to multiply Eq. (2) by m^2 . The equation for steady state then becomes

$$0 = \nabla \cdot A \nabla f^0 + c_1 \frac{\partial f^0}{\partial \epsilon} + c_2 \frac{\partial f^0}{\partial z} + c_3 f^0, \quad (10)$$

where

$$A = \frac{8\pi\epsilon}{3NQ} \begin{bmatrix} E^2 + (6mN^2\epsilon Q^2 k T / M 10^7 e) & E \\ E & 1 \end{bmatrix}, \quad (12)$$

$$c_1 = \frac{16Nm\pi\epsilon^2 Q}{M} - \frac{8\pi\epsilon e}{3Q} \frac{\partial E}{\partial z} \frac{1}{N}, \quad (13)$$

$$c_2 = \frac{8\pi\epsilon}{3Q} \frac{\partial}{\partial z} \frac{1}{N}, \quad c_3 = \frac{\partial c_1}{\partial \epsilon}. \quad (14)$$

Note that the problem has been somewhat equilibrated and

$$A \sim \epsilon \begin{bmatrix} 10^{-1} + 10^{-3} \epsilon T & 10^{-1} \\ 10^{-1} & 10^{-1} \end{bmatrix}. \quad (15)$$

We assume that the domain of definition of the partial differential equation (10) is $\mathcal{R} \equiv [0, \bar{\epsilon}] \times [0, \bar{z}]$ and that ϵ/Q is bounded in \mathcal{R} . The cross section $Q(\epsilon) > 0$ and hence Eq. (10) is *elliptic* for $T > 0$ (and *parabolic* for $T = 0$) on the interior of \mathcal{R} since

$$\det A = 16\pi Nm k \epsilon^2 Q T / M 10^7 e.$$

Unfortunately, Eq. (10) is *non-self-adjoint* [9, p. 167], a property which tends to foster *nonsymmetric* finite difference models. In addition, the non-self-adjointness of (10) precludes the use of Ritz or finite element techniques due to the absence of a variational principle. Even though (10) is *essentially self-adjoint* [10, p. 103], the transformations involved to simplify the equation are quite complex and unwieldy, so too are the standard transformations for removal of the cross-derivative terms

$\partial^2 f / \partial \epsilon \partial z$ [11, p. 46]. We conclude that (10) is a nonmodel partial differential equation, the numerical solution of which requires somewhat novel applications of various tools of numerical analysis.

The boundary conditions imposed are

$$\left. \begin{aligned}
 f^0 &= 0, & \epsilon &= \bar{\epsilon}, & 0 &\leq z \leq \bar{z}, \\
 f^0 &= 0, & 0 &\leq \epsilon \leq \bar{\epsilon}, & z &= \bar{z}, \\
 E \frac{\partial f^0}{\partial \epsilon} + \frac{\partial f^0}{\partial z} &= 0, & \epsilon &= 0, & 0 &\leq z \leq \bar{z}, \\
 f^0 &= \exp \left\{ \int_0^\epsilon \frac{P(\epsilon) d\epsilon}{1 + (kT/10^7 e) P(\epsilon)} \right\}, & 0 &\leq \epsilon \leq \bar{\epsilon}, & z &= 0,
 \end{aligned} \right\} \quad (16)$$

where

$$P(\epsilon) = (6mN^2/ME^2)[Q(\epsilon)]^2 \epsilon.$$

The boundary condition at $z = 0$ is simply the value of f^0 obtained from assuming all gradient terms in z are zero, appropriate to a position in the electron stream far from the absorbing boundary. The boundary condition at $\epsilon = 0$ is obtained from (2) by requiring that $\partial f^0 / \partial t$ be finite at $\epsilon = 0$, it being assumed that $Q(0)$ is always finite and greater than zero.

In the next section, a finite difference model of (10) and (16) is described. Once the electron distribution function f^0 is approximated, the *electron current density* and *electron density* can be expressed in terms of f^0 as, respectively [5],

$$\begin{aligned}
 \Gamma(\bar{r}, t) &= \frac{-8\pi}{3m^2N} \int_0^{\bar{\epsilon}} \frac{\epsilon}{Q} \left(-\frac{\partial^2 f^0}{\partial z^2} + eE \frac{\partial f^0}{\partial \epsilon} \right) d\epsilon, \\
 n(\bar{r}, t) &= \frac{4\pi}{m} \left(\frac{2}{m} \right)^{1/2} \int_0^{\bar{\epsilon}} \epsilon^{1/2} f^0 d\epsilon.
 \end{aligned} \quad (17)$$

3. FINITE DIFFERENCE MODEL

The non-self-adjoint nature of (10) fosters a *nonsymmetric* system of finite difference equations of the form

$$\mathcal{A}\bar{F} = \bar{k}, \quad (18)$$

where we choose a view \mathcal{A} as a perturbation of a *symmetric* matrix \mathcal{A}_1 . That is, $\mathcal{A} = \mathcal{A}_1 + \mathcal{A}_2$, $\mathcal{A}_1^T = \mathcal{A}_1$, and \mathcal{A}_2 is "small" in norm.

Consider the finite difference mesh π as indicated in Fig. 1. Each equation in (18) represents an approximation to (10) at a mesh point of π . In the light of the boundary conditions (16) we deduce that the dimension of \mathcal{A} is $d \times d$, where $d = (NZ - 2)(NE - 1)$ and for our experiments $750 \leq d \leq 7500$.

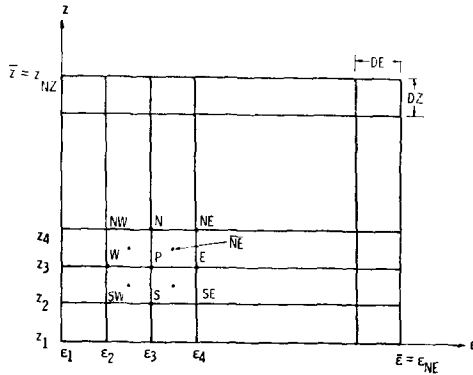


FIG. 1. Rectangular mesh π of gauge $H = \max\{DE, DZ\}$.

As indicated in Fig. 1, a point of the grid and its eight closest neighbors are referred to generically according to compass designations (cf. Forsythe and Wasow [9, p. 185]). The coefficients $\overline{A}_{ij}(\epsilon, z)$ are evaluated at *centroids* of mesh cells designated, respectively, \overline{NW} , \overline{NE} , \overline{SW} , \overline{SE} so as to preserve *symmetry* of the second-order operator $(\nabla \cdot A\nabla)$ and hence to reduce storage requirements and hopefully to enhance convergence of iterative schemes.

The following result does not seem to be readily available in the literature and is included for completeness.

If U is sufficiently differentiable,

$$(\partial U / \partial \epsilon)(P) = (4DE)^{-1}[U(NE) + U(SE) - U(NW) - U(SW)] + O(H^2), \quad (19)$$

$$(\partial U / \partial z)(P) = (4DZ)^{-1}[U(NE) - U(SE) + U(NW) - U(SW)] + O(H^2) \quad (20)$$

as $H = \max\{DE, DZ\} \rightarrow 0$. The verification of (19) and (20) follows from standard Taylor series arguments. Note that in the case of (19) [(20)] the term involving U_{zzz} [$U_{\epsilon\epsilon\epsilon}$] also drops out on the right-hand side, which avoids ratios of the type DZ/DE [DE/DZ].

To discretize the differential operator in (10) at the generic mesh point P , we first apply (19) and (20) with (SW, SE, P, NW, NE) replaced by $(\overline{SW}, \overline{SE}, P, \overline{NW}, \overline{NE})$ as follows.

$$\begin{aligned} \frac{\partial}{\partial \epsilon} \left[A_{11} \frac{\partial f^0}{\partial \epsilon} + A_{12} \frac{\partial f^0}{\partial z} \right] &= (4 DE)^{-1} \left[A_{11}(\overline{NE}) \frac{\partial f^0}{\partial \epsilon} (\overline{NE}) + A_{12}(\overline{NE}) \frac{\partial f^0}{\partial z} (\overline{NE}) \right. \\ &\quad + A_{11}(\overline{SE}) \frac{\partial f^0}{\partial \epsilon} (\overline{SE}) + A_{12}(\overline{SE}) \frac{\partial f^0}{\partial z} (\overline{SE}) \\ &\quad - A_{11}(\overline{NW}) \frac{\partial f^0}{\partial \epsilon} (\overline{NW}) - A_{12}(\overline{NW}) \frac{\partial f^0}{\partial z} (\overline{NW}) \\ &\quad \left. - A_{11}(\overline{SW}) \frac{\partial f^0}{\partial \epsilon} (\overline{SW}) - A_{12}(\overline{SW}) \frac{\partial f^0}{\partial z} (\overline{SW}) \right], \quad (21) \end{aligned}$$

and a similar expression approximating $(\partial/\partial z)[A_{21}(\partial f^0/\partial \epsilon) + A_{22}(\partial f^0/\partial z)]$. These approximations in turn necessitate approximating $\partial f^0/\partial \epsilon$ and $\partial f^0/\partial z$ at the centroids \overline{NE} , \overline{SE} , \overline{NW} , and \overline{SW} , and again the finite difference approximation in (19) and (20) are applied with $(\overline{SW}, \overline{SE}, P, \overline{NW}, \overline{NE})$ being replaced by, for example, $(P, E, \overline{NE}, N, \overline{NE})$.

The coefficients $c_1(P)$ and $c_2(P)$ are approximated by an arithmetic average of the values of c_1 and c_2 (resp.) at the four neighboring centroids. Hence, the functions N , Q , and E need only be specified at centroids. The linear terms $\partial f^0/\partial \epsilon(P)$, $\partial f^0/\partial z(P)$, etc., are also approximated using (19) and (20).

Following the above discretization procedure, the differential equation (10) is approximated at each mesh point P by the finite difference equation

$$L_h(F^0) = \sum_Q A(P, Q) F^0(Q) = 0, \tag{22}$$

where at most nine couplings $A(P, Q)$ are nonzero. These couplings are tabulated in the Appendix.

So far we have not established an ordering of the mesh points in π . Let $P_{ij} : (\epsilon_i, z_j)$, $F_{ij}^0 = F^0(P_{ij})$ and partition the unknown vector $\bar{F} = (\bar{F}_1, \bar{F}_2, \dots, \bar{F}_{NZ-2})^T$, where $\bar{F}_j = (F_{1,j+1}^0, F_{2,j+1}^0, \dots, F_{NE-1,j+1}^0)^T$, $1 \leq j \leq NZ - 2$. The unknowns are in this way ordered from left to right, a row at a time, and from the bottom row to the top row.

\mathcal{O}_2 is taken to be the matrix containing only those components of the couplings $A(P, Q)$ designated by EX and EZ in the formulas given in the Appendix. That is, \mathcal{O}_2 is the discretization of the linear terms $c_1(\partial f^0/\partial \epsilon)$ and $c_2(\partial f^0/\partial z)$ while $\mathcal{O}_1 \equiv \mathcal{O} - \mathcal{O}_2$ is the discretization of $\nabla \cdot A \nabla f^0 + c_3 f^0$.

We remark that \mathcal{O}_1 is *symmetric* by design. For example,

$$[\mathcal{O}_1]_{34} = A(P_{32}, E) = A(P_{42}, W) = [\mathcal{O}_1]_{43}.$$

The evaluation of the energy- and space-dependent coefficients of the partial differential equation at the centroids of mesh cells is crucial for this symmetry to manifest itself.

4. ITERATIVE SCHEME

Various iterative schemes (block Jacobi, block Gauss-Seidel, block SOR, etc. [9]) were implemented in an attempt to solve the finite difference model (22) efficiently. Not all the attempts were successful since the matrix \mathcal{O} fails to conform to the characteristics of matrices typical of more model boundary value problems. The iteration matrices considered apparently are *not monotone* (and hence *not of*

positive type [9, p. 181]), a property often very useful in establishing convergence behavior of the iterative scheme as well as theoretical convergence of the finite difference model [12, 3]. This was observed by numerical experimentation on several test problems. The "nonmodelness" of the linear system (18) or (22) stems from two sources: (i) the presence of the cross-derivative term $\epsilon^2 f / \partial \epsilon \partial z$, whose discretization yields difference equations which are not of positive type, and (ii) the *asymmetry* induced by the first-order terms $\partial f^0 / \partial \epsilon$ and $\partial f^0 / \partial z$.

The analysis of any iterative scheme applied to (22) is also compounded by the presence of variable coefficients in the partial differential equation which vary from problem to problem and which may be singular (e.g., for $Q(\epsilon) \propto \epsilon^{4/3}$ at $\epsilon = 0$).

The matrix \mathcal{A} is block tridiagonal, (and hence consistently ordered 2 cyclic [13, p. 102]) and the block Gauss-Seidel iterates will converge *asymptotically* twice as fast as the block Jacobi iterates [13, p. 108], assuming either converges.

We next describe the *block Gauss-Seidel* iterative scheme which has worked well for those problems considered to date. The linear system (18) is partitioned (to be consistent with the partitioning of \bar{F} given in the previous section) as

$$\mathcal{A}\bar{F} = \begin{bmatrix} \mathcal{A}_{11} & \mathcal{A}_{12} & & & \circ \\ \mathcal{A}_{21} & \mathcal{A}_{22} & \mathcal{A}_{23} & & \\ & \diagdown & \diagdown & \diagdown & \\ & & & \mathcal{A}_{NZ-3, NZ-2} & \\ \circ & & & \mathcal{A}_{NZ-2, NZ-2} & \\ \mathcal{A}_{NZ-2, NZ-3} & & & & \end{bmatrix} \begin{bmatrix} \bar{F}_1 \\ \bar{F}_2 \\ \cdot \\ \cdot \\ \cdot \\ \bar{F}_{NZ-2} \end{bmatrix} = \begin{bmatrix} \bar{K}_1 \\ 0 \\ \cdot \\ \cdot \\ 0 \\ \bar{K}_{NZ-2} \end{bmatrix}, \tag{23}$$

where \bar{F}_j contains the unknowns $F_{i,j+1}^0$ in the row of mesh points along $z = z_{j+1}$ (ordered left to right). Define

$$\mathcal{D} = \text{Block-diag}\{\mathcal{A}_{11}, \mathcal{A}_{22}, \dots, \mathcal{A}_{NZ-1, NZ-1}\} \tag{24}$$

and

$$\mathcal{B} = \mathcal{D}^{-1}\mathcal{A} = I + L + R, \tag{25}$$

where L is strictly lower triangular and R is strictly upper triangular. Then system (23) is equivalent to

$$\mathcal{B}\bar{F} = \mathcal{K} \equiv [\mathcal{A}_{11}^{-1}\bar{K}_1, 0, \dots, 0, \mathcal{A}_{NZ-1, NZ-1}^{-1}K_{NZ-2}]^T, \tag{26}$$

where we have used the fact that

$$\mathcal{A}_{ii} = \text{Tridiag}\{A(P, W), A(P, P), A(P, E)\}$$

is *strictly diagonally dominant* from the appendix and hence nonsingular.

The *point Gauss-Seidel* iteration scheme for (26), or equivalently the *block Gauss-Seidel* scheme for (23), is given by

$$\bar{F}^{(k+1)} = -(I + R)^{-1}L\bar{F}^{(k)} + (I + R)^{-1}\mathcal{K} \tag{27}$$

($k = 0, 1, \dots$). The roles of R and L can of course be interchanged in (27) to obtain a variation on (27). $J = -(I + R)^{-1}L$ is termed the *Gauss-Seidel iteration matrix*, and it is known [11, p. 80] that under the *assumption* that \mathcal{B} (or equivalently \mathcal{O}) is symmetric, (27) converges to \bar{F} as $k \rightarrow \infty$ if and only if \mathcal{B} (or \mathcal{O}) is positive definite. But unfortunately, our \mathcal{O} is *not* symmetric.

However, as indicated in Section 3, \mathcal{O} is “close to” the *symmetric* matrix \mathcal{O}_1 (equivalently, \mathcal{B} is “close to” $\mathcal{D}^{-1}\mathcal{O}_1$) and by continuity we expect the iteration matrices associated with \mathcal{O} and \mathcal{O}_1 to behave in a similar fashion. Stein [14] has established conditions for convergence in such nonsymmetric cases. Suffice it to say that in our case $\mathcal{O} \rightarrow \mathcal{O}_1$ as $H \rightarrow 0$ and, assuming $\|\mathcal{O}^{-1}\|_\infty$ is bounded as $H \rightarrow 0$, the conditions given in [9] are very reasonable.

The implementation of (27) is accomplished by solving for $\bar{F}^{(k+1)}$ a row at a time via

$$\mathcal{O}_{NZ-1, NZ-1}\bar{F}_{NZ-1}^{(k+1)} = -\mathcal{O}_{NZ-1, NZ-2}\bar{F}^{(k)} + \bar{K}_{NZ-1}, \tag{28}$$

$$\mathcal{O}_{jj}\bar{F}_j^{(k+1)} = -\mathcal{O}_{jj-1}\bar{F}^{(k)} - \mathcal{O}_{jj+1}\bar{F}^{(k+1)} + \bar{K}_j, \quad j = NZ - 2, \quad NZ - 3, \dots, 1,$$

where the tridiagonal systems in (28) are solved using the factorization technique given, for example, in [13, p. 195].

Acceleration of convergence for the sequence in (27) was desirable since, as indicated in the next section, for some problems considered, a large number of iterations were required to achieve the desired accuracy. Successive over relaxation (SOR) was considered, and we sought a parameter ω such that the iterates

$$\bar{F}^{(k+1)} = (1 - \omega)\bar{F}^{(k)} + \omega\bar{F}_1^{(k+1)} \quad (k = 0, 1, \dots) \tag{29}$$

converged in some sense faster than the sequence in (27). In (29), $\bar{F}_1^{(k+1)}$ is the Gauss-Seidel iterate from (28) based on $\bar{F}^{(k)}$ and components of $\bar{F}^{(k+1)}$ as they are computed. The value of $\omega = 1$ in (29) yields the Gauss-Seidel scheme identically.

In light of [13, Theorem 4.4] a reasonable choice of the acceleration parameter is

$$\omega = 2/[1 + (1 - \rho)^{1/2}], \tag{30}$$

where ρ is the spectral radius of the Gauss-Seidel matrix J . The power method [13, p. 291] was used to estimate ρ and we discovered that an apparent manifestation of the asymmetry of J is the absence of an eigenvalue equal to ρ . That is, the power method did not converge.

To circumvent this problem, the power method was used to estimate the spectral radius, ρ_1 , of the Gauss-Seidel matrix associated with \mathcal{O}_1 , and ρ_1 used as an estimate to ρ in (30). The basic program is easily modified to implement this strategy. First, the terms EX and EZ (cf. Appendix) are equated to zero (transforming \mathcal{O} into \mathcal{O}_1), and second, the boundary data are set to zero. In (28), the \bar{K}_j are all zero and (28) reduces to the desired power method to estimate ρ_1 and its eigenvector. After ρ_1 is estimated, the boundary data, EX and EZ terms are reinitialized and the basic iterative (28)–(29) is begun.

5. A NUMERICAL EXAMPLE

We have obtained solutions for a number of physical conditions, for various values of the parameters of pressure, electric field, temperature, and form of the cross section Q , including cases of back diffusion where electrons diffuse against the electric field.

In the present paper we give only one illustrative example, i.e., the case where $E/N = 10^{-17}$ V cm², $p = 3$ Torr, $T = 293$ K, for a gas of atomic weight 4. Other parameters of Eq. (2) involve the usual physical constants, i.e., $m = 9.11 \times 10^{-28}$ g, $M = 6.68 \times 10^{-24}$ g, and $k = 1.38 \times 10^{-23}$ J/K. The cross section $Q(\epsilon)$ was set equal to 60ϵ cm², where ϵ is in eV.

The solution corresponds to the physical situation of a continuous stream of electrons over an infinite plane being subjected to a uniform electric field of strength 0.99 V/cm and being collected by a metal electrode. The metal electrode absorbs electrons and is assumed to impose an effective boundary condition of zero on f^0 . In the immediate vicinity of the boundary there are large gradients in f^0 . However, at a distance sufficiently far from the boundary, f^0 will be independent of z . The distance from the metal boundary at which f^0 is effectively independent of z was determined by several trial solutions.

The derived distribution function $f^0(\epsilon, z)$ illustrated by the solid curve in Fig. 2 for $NZ = 49$ and $NE = 119$ ($DZ = 0.0125$ cm and $DE = 0.005$ eV). The absorbing metal boundary is at $z = 1.2$ cm, where $f^0(\epsilon, 1.2) = 0$. The curve for $z = 0.6$ cm is the solution for f^0 , with all gradient terms in z of (2) omitted, imposed as a boundary value. A similar solution for $f_0^0(\epsilon, z)$ with z ranging from 0 to 1.2 cm showed that between $z = 0$ and 0.6 the derived values of f^0 differ insignificantly from the solution with all gradient terms in z omitted. Also shown in Fig. 2 are solutions with coarser mesh sizes, i.e., (i) $DE = 0.005$, $DZ = 0.025$, and (ii) $DE = 0.01$ and $DZ = 0.05$. It is seen that at low energies numerical results are sensitive to the mesh size near the absorbing boundary at 1.2 cm.

However, this sensitivity to the mesh size is much less severe on the calculated values of electron density, shown in Fig. 3. It is this integral over f^0 which is the

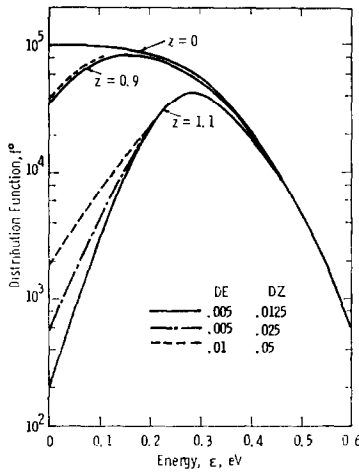


FIG. 2. Derived electron distribution function $f^0(\epsilon, z)$. At $z = 1.2$ cm an absorbing electrode imposes a boundary condition $f^0 = 0$.

more significant physical quantity in most problems. Also shown in Fig. 3 is the electron density obtained by the conventional [4, 5] solution of the electron continuity equation, i.e.,

$$\frac{\partial}{\partial z} \left(nW - D \frac{\partial n}{\partial z} \right) = 0,$$

where W and D are taken as independent of z ; W is the electron drift velocity and D the electron diffusion coefficient evaluated from f^0 obtained from (2) where density gradients are neglected. It is seen that the usual treatment of diffusion is con-

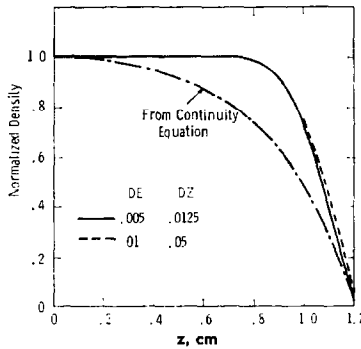


FIG. 3. Calculated electron density compared with a classical solution from the continuity equation where drift and diffusion coefficients are assumed independent of z .

siderably in error from the more complete analysis given in the present paper. Thus the spatial gradients terms of (2) are significant, particularly near boundaries where density gradients are large.

In Fig. 4 we illustrate the significant improvement in the rate of convergence of the solution of f^0 by the use of our procedure to select an optimum of ω . Using $\omega = 1.789$, evaluated from this procedure, the solution had effectively converged after 270 iterations, the maximum variation of any value of f^0 being <1 . For $\omega = 1$ however, variations in f^0 at each iteration after 1000 iterations were 2 orders of magnitude higher.

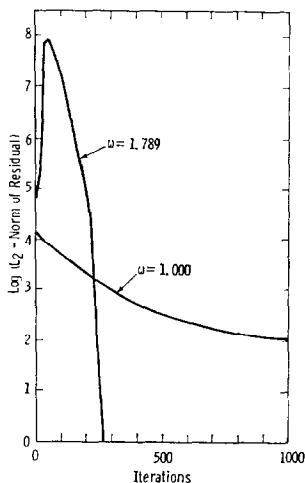


FIG. 4. Behavior of $\|\bar{F}^{(k+1)} - \bar{F}^{(k)}\| = (\sum_{k=1}^d (\bar{F}^{(k+1)} - \bar{F}^{(k)})^2)^{1/2}$, where $d = 5546$.

Further checks on the numerical accuracy of the solution are as follows.

(1) The derived values of electron density are equal, to within 5%, with the solution derived independently using a different explicit numerical procedure of solving (2), which was a relaxation method based upon the time dependence of f^0 given in (2). The explicit procedure however, needed larger computation times of more than an order of magnitude.

(2) The derived values of $W = 2.58 \cdot 10^5$ cm/sec and $D = 8.40 \cdot 10^4$ cm²/sec for $z = 0.6$ cm are in good agreement with values of $W = 2.78 \times 10^5$ cm/sec and $D = 8.77 \cdot 10^4$ cm²/sec derived from the analytic formula obtained from Ref. [5, Eqs. (3), (5) and (6)], using the variation of Q with energy of $Q = 60\epsilon$, but with $T = 0$ K instead of 293 K.

(3) A consequence of integrating (2) over energy is that electron flux should be constant with z . We have evaluated the electron flux from [Ref. 5, Eq. (18)] as a

check on our calculations and found that the flux is constant to 3%, for all values of z .

(4) The iterative logic and the computer program were checked by solving a problem involving Laplace's equation for which an exact solution is known.

6. SUMMARY

The second-order differential equation defining the electron distribution function f^0 , derived from the Boltzmann transport equation, has variable coefficients and also a term in $\partial^2 f^0 / \partial \epsilon \partial z$ which is not easily handled by standard finite difference schemes. A further complication is the asymmetry of the partial differential equation which necessarily fosters a nonsymmetric set of difference equations. A somewhat novel finite difference model has been devised which is "almost" symmetric and which yields efficient iterative solutions. Significant differences are obtained between numerical solutions using the present method and conventional diffusion methods which ignore the effect of density gradients on the distribution function.

APPENDIX: FINITE DIFFERENCE COUPLINGS

$$\begin{aligned}
 A(P, P) = & (1/4DE^2)\{-A_{11}(\overline{NE}) - A_{11}(\overline{SE}) - A_{11}(\overline{NW}) - A_{11}(\overline{SW})\} \\
 & + (2/4DEDZ)\{-A_{12}(\overline{NE}) + A_{12}(\overline{SE}) - A_{12}(\overline{NW}) - A_{12}(\overline{SW})\} \\
 & + (1/4DZ^2)\{A_{22}(\overline{NE}) - A_{22}(\overline{SE}) - A_{22}(\overline{NW}) - A_{22}(\overline{SW})\} \\
 & + (1/2DE)\{c_1(\overline{NE}) + c_1(\overline{SE}) - c_1(\overline{NW}) - c_1(\overline{SW})\}
 \end{aligned}$$

$$A(P, E) = \frac{1}{4DE^2} \{A_{11}(\overline{NE}) + A_{11}(\overline{SE})\} + \frac{1}{4DZ^2} \{-A_{22}(\overline{NE}) - A_{22}(\overline{SE})\}$$

$$A(P, N) = \frac{1}{4DE^2} \{-A_{11}(\overline{NE}) - A_{11}(\overline{NW})\} + \frac{1}{4DZ^2} \{A_{22}(\overline{NE}) + A_{22}(\overline{NW})\}$$

$$A(P, S) = \frac{1}{4DE^2} \{-A_{11}(\overline{SE}) - A_{11}(\overline{SW})\} + \frac{1}{4DZ^2} \{A_{22}(\overline{SE}) + A_{22}(\overline{SW})\}$$

$$A(P, W) = \frac{1}{4DE^2} \{A_{11}(\overline{NW}) + A_{11}(\overline{SW})\} + \frac{1}{4DZ^2} \{-A_{22}(\overline{NW}) - A_{22}(\overline{SW})\}$$

$$A(P, NW) = \frac{A_{11}(\overline{NW})}{4DE^2} + \frac{A_{22}(\overline{NW})}{4DZ^2} - \frac{A_{12}(\overline{NW})}{2DEDZ} - EX + EZ$$

$$A(P, NE) = \frac{A_{11}(\overline{NE})}{4DE^2} + \frac{A_{22}(\overline{NE})}{4DZ^2} + \frac{A_{12}(\overline{NE})}{2DEDZ} + EX + EZ$$

$$A(P, SW) = \frac{A_{11}(\overline{SW})}{4DE^2} + \frac{A_{22}(\overline{SW})}{4DZ^2} + \frac{A_{12}(\overline{SW})}{2DEDZ} - EX - EZ$$

$$A(P, SE) = \frac{A_{11}(\overline{SE})}{4DE^2} + \frac{A_{22}(\overline{SE})}{4DZ^2} - \frac{A_{12}(\overline{SE})}{2DEDZ} + EX - EZ$$

$$EX = [c_1(\overline{NW}) + c_1(\overline{NE}) + c_1(\overline{SE}) + c_1(\overline{SW})]/16 DE$$

$$EZ = [c_2(\overline{NW}) + c_2(\overline{NE}) + c_2(\overline{SE}) + c_2(\overline{SW})]/16 DZ$$

ACKNOWLEDGMENTS

This work was supported by NSF in a Faculty Research Participation grant. We are also appreciative of assistance from D. P. Wei, of the computer science department.

REFERENCES

1. W. P. ALLIS, in "Handbuch der Physik," Vol. 21 (S. Flügge, Ed.) Springer-Verlag, Berlin, 1956.
2. L. G. H. HUXLEY AND R. W. CROMPTON, "The Diffusion and Drift of Electrons in Gases," Wiley, New York, 1974.
3. L. S. FROST AND A. V. PHELPS, *Phys. Rev.* **127** (1962), 1621.
4. J. J. LOWKE, *Austral. J. Phys.* **26** (1973), 469.
5. J. H. PARKER, JR., AND J. J. LOWKE, *Phys. Rev.* **181** (1969), 290.
6. H. R. SKULLERUD, *J. Phys. B* **2** (1969), 696.
7. J. LUCAS AND H. T. SAELEE, *J. Phys. D* **8** (1975), 640.
8. R. E. ROBSON AND K. KUMAR, *Austral. J. Phys.* **24** (1971), 835.
9. G. FORSYTHE AND W. WASOW, "Difference Methods for Partial Differential Equations," Wiley, New York, 1960.
10. W. F. AMES, "Numerical Methods for Partial Differential Equations," Barnes and Noble, New York, 1969.
11. H. F. WEINSTEIN, "A First Course in Partial Differential Equations," p. 46, Blaisdell, New York, 1965.
12. J. H. BRAMBLE AND B. E. HUBBARD, *Math. Comp.* **18** (1964), 349.
13. R. S. VARGA, "Matrix Iterative Analysis," Prentice-Hall, Englewood Cliffs, N.J., 1962.
14. P. STEIN, *Math. Comp.* **5** (1951), 237.